Neurospine 2024;21(2):606-619.
https://doi.org/10.14245/ns.2347330.665

Neurospine
pISSN 2586-6583 eISSN 2586-6591

Original Article

Corresponding Author
Yong Hai
https://orcid.org/0000-0002-7206-325X

Department of Orthopedic Surgery, Beijing Chaoyang Hospital, Capital Medical University, GongTiNanLu 8#, Chaoyang District, Beijing 100020, China
Email: prof.haiyong@yahoo.com

Co-Corresponding Author
Peng Yin
https://orcid.org/0000-0001-9984-7663

Department of Orthopedic Surgery, Beijing Chaoyang Hospital, Capital Medical University, GongTiNanLu 8#, Chaoyang District, Beijing 100020, China
Email: yinpeng3904@126.com

Received: December 17, 2023
Revised: February 17, 2024
Accepted: February 17, 2024

*Weishi Liang and Yihan Yang contributed equally to this study as co-first authors.

Biomechanical Analysis of Hybrid Artificial Discs or Zero-Profile Devices for Treating 1-Level Adjacent Segment Degeneration in ACDF Revision Surgery

Weishi Liang[1,2,3,*], Yihan Yang[1,2,3,*], Bo Han[1,2,3], Duan Sun[1,2,3], Peng Yin[1,2,3], Yong Hai[1,2,3]

[1]Department of Orthopedic Surgery, Beijing Chaoyang Hospital, Capital Medical University, Beijing, China
[2]Joint Laboratory for Research and Treatment of Spinal Cord Injury in Spinal Deformity, Laboratory for Clinical Medicine, Capital Medical University, Beijing, China
[3]Center for Spinal Deformity, Capital Medical University, Beijing, China

Objective: Cervical hybrid surgery optimizes the use of cervical disc arthroplasty (CDA) and zero-profile (ZOP) devices in anterior cervical discectomy and fusion (ACDF) but lacks uniform combination and biomechanical standards, especially in revision surgery (RS). This study aimed to investigate the biomechanical characteristics of adjacent segments of the different hybrid RS constructs in ACDF RS.
Methods: An intact 3-dimensional finite element model generated a normal cervical spine (C2–T1). This model was modified to the primary C5–6 ACDF model. Three RS models were created to treat C4–5 adjacent segment degeneration through implanting cages plus plates (Cage-Cage), ZOP devices (ZOP-Cage), or Bryan discs (CDA-Cage). A 1.0-Nm moment was applied to the primary C5–6 ACDF model to generate total C2–T1 range of motions (ROMs). Subsequently, a displacement load was applied to all RS models to match the total C2–T1 ROMs of the primary ACDF model.
Results: The ZOP-Cage model showed lower biomechanical responses including ROM, intradiscal pressure, maximum von Mises stress in discs, and facet joint force in adjacent segments compared to the Cage-Cage model. The CDA-Cage model exhibited the lowest biomechanical responses and ROM ratio at adjacent segments among all RS models, closely approached or lower than those in the primary ACDF model in most motion directions. Additionally, the maximum von Mises stress on the C3–4 and C6–7 discs increased in the Cage-Cage and ZOP-Cage models but decreased in the CDA-Cage model when compared to the primary ACDF model.
Conclusion: The CDA-Cage construct had the lowest biomechanical responses with minimal kinematic change of adjacent segments. ZOP-Cage is the next best choice, especially if CDA is not suitable. This study provides a biomechanical reference for clinical hybrid RS decision-making to reduce the risk of ASD recurrence.

Keywords: Biomechanical analysis, Cervical revision surgery, Hybrid surgery, Adjacent segment degeneration, Zero-profile device, Cervical disc arthroplasty

INTRODUCTION

Adjacent segment degeneration (ASD) is a commonly observed long-term complication in middle-aged and elderly patients who have undergone cervical fusion.[1] The main manifestations on imaging are disc height reduction and herniation, facet joint proliferation, and segmental instability. When a patient exhibits neurological symptoms that correspond to imag-

ing findings of ASD, it is referred to as adjacent segment disease.[1] Studies have reported varying incidence rates of ASD, ranging from 16% to 96%, with an average incidence of approximately 47.33%.[2] It has been observed that an increased number of fusion segments can accelerate the development of ASD following anterior cervical discectomy and fusion (ACDF).[3] ACDF has gradually developed into the standard procedure for anterior cervical fusion since the 1950s. Risk factors associated with the progression of ASD include biomechanical factors, fixation plate length, screw insertion angle, cervical dislocation sequence, age, and other factors.[4,5] Among these, biomechanical factors are considered the most significant contributors to the development of ASD.[6] ASD disrupts the biomechanical stability of the cervical spine, and in cases of severe nerve compression, surgical revision becomes necessary to address the condition.

However, for patients with secondary ASD after primary ACDF surgery, traditional titanium alloy cages plus plates are still conventionally used in revision surgery (RS).[7] Segmental fusion in these cases leads to a greater loss of motor segments, an increase in range of motion (ROM) compensation, and an elevated risk of ASD.[4,8] The novel zero-profile (ZOP) device has been gradually applied in ACDF surgery. The ZOP device is superior to cage plus plate in reducing the incidence of ASD, minimizing intraoperative blood loss, and alleviating dysphagia.[9] Moreover, a finite element (FE) study also reported that the ZOP device effectively reduces biomechanical responses by reducing the ROM and intradiscal pressure (IDP) in the nucleus pulposus at adjacent segments.[10]

In recent years, anterior cervical hybrid surgery developed rapidly as an innovative approach to treat multi-segmental cervical degeneration disease (CDD).[11] This procedure combines ACDF with cervical disc arthroplasty (CDA), providing a new strategy for RS after ACDF.[11] The implantation of an artificial disc in the cervical spine can improve the distribution ratio of intervertebral ROM to a certain extent by preserving motion in the surgical segments.[12,13] Furthermore, many biomechanical studies have demonstrated that hybrid surgery surpasses ACDF surgery in restoring the normal biomechanical state of the cervical spine.[12,14]

It is well recognized that the significant increase in IDP and facet joint force (FJF) caused by the compensatory increase in the ROM of the upper and lower adjacent segments after ACDF serves as a critical biomechanical mechanism underlying ASD.[15] The RS strategy for the ASD following ACDF necessitates a reconstruction of the cervical spine sequence and a reduction in the biomechanical responses of adjacent segments. The hybrid strategies used in the treatment of multilevel CDDs are diversified, mostly based on the surgical experience of surgeons, and lack of strong biomechanical and long-term follow-up evidence. Particularly in RS, there is a deficiency in biomechanical data as a reference for making surgical decisions and forecasting the long-term degenerative prognosis of adjacent segments. Both the ZOP device and the cervical artificial disc exhibit the capability to reduce the biomechanical responses on adjacent segments. However, their effectiveness in reducing the biomechanical responses of adjacent segments and reducing the risk of ASD recurrence compared with traditional ACDF revision has not been reported, and further investigation is needed.

In this study, we established the C2–T1 intact, primary ACDF model, and 3 other RS FE models integrating previous ACDF procedures with new-implanted revision devices: the traditional cage plus plate (Cage-Cage), the ZOP device (ZOP-Cage), and the Bryan disc (CDA-Cage) models. These FE models were designed to explore the biomechanical characteristics of adjacent segments in the RS models. From the biomechanical perspective, this FE study will provide a basis for selecting suitable RS methods to reduce the risk of ASD recurrence following ACDF RS.

MATERIALS AND METHODS

1. Establishment of the Intact Cervical FE Model

The geometric model of the C2–T1 vertebrae was generated using computed tomography (CT) scan data derived from the cervical spine of a healthy 30-year-old female, as illustrated in Fig. 1. Initial processing of the CT scan data involved its importation into Mimics (Materialise Inc., Leuven, Belgium), where

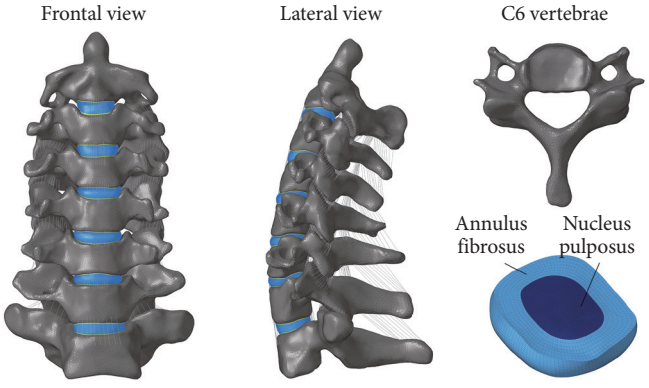

Fig. 1. Three-dimensional structural illustrations of intact C2–T1 finite element model. A frontal and lateral view of the finite element model, C6 vertebrae, and disc structure were shown.

Table 1. Material properties of the cervical finite element model

Component	Element type	Constitutive model	Young's modulus (MPa)	Poisson ratio	Reference
Cortical bone	C3D4 C3D8	Isotropic elastic	E = 10,000	ν = 0.3	18
Cancellous bone	C3D4	Neo-Hookean	E = 100	ν = 0.3	20
Annulus ground substance	C3D8H	Mooney-Rivlin	C_{10} = 0.1333, C_{01} = 0.0333, D_1 = 0.6	-	20
Annulus fibers	T3D2	Hypeoelastic	350–550	ν = 0.3	17
Nucleus pulposus	C3D8H	Mooney-Rivlin	C_{10} = 0.12, C_{01} = 0.09, D_1 = 0	-	13
Spine ligaments (ALL, PLL, ISL, LF, CL)	Spring	Nonlinear elastic	-	-	19
PEEK cage	C3D4	Linear elastic	E = 3,760	ν = 0.38	17
Screws/plate (titanium alloy)	C3D4	Linear elastic	E = 110,000	ν = 0.3	7
PEEK ZOP device	C3D4	Linear elastic	E = 3,760	ν = 0.38	4, 17
ZOP device screws (titanium alloy)	C3D4	Linear elastic	E = 110,000	ν = 0.3	7
Bryan disc shell	C3D8	Linear elastic	E = 110,000	ν = 0.3	35
Bryan disc Nucleus	C3D8	Linear elastic	E = 30	ν = 0.45	35

ALL, anterior longitudinal ligament; PLL, posterior longitudinal ligament; ISL, interspinous ligament; LF, ligamentum flavum; CL, capsular ligament; PEEK, polyetheretherketone; ZOP, zero-profile.

it was converted into a geometric structure. The resulting geometric model was then subjected to meshing procedures using Hypermesh (Altair Engineering Inc., Troy, MI, USA). Subsequently, the meshed model underwent preprocessing and analysis using Abaqus (Dassault Systemes Simulia Corp., Johnston, RI, USA). The FE study protocol has been reviewed and approved by the Ethics Committee of Beijing Chaoyang Hospital, Capital Medical University (No. 2019-ke-212).

2. Material Properties and FE Modeling

The material properties utilized in this study's FE models followed previously published literature, and the detailed information was summarized in Table 1. The vertebrae were divided into 2 regions: cortical bone (1-mm thickness) and cancellous bone, both meshed using tetrahedral elements.[16,17] The cortical endplates of the discs and facet joints were meshed with hexahedral elements. Furthermore, the intervertebral disc was divided into 3 components: the nucleus pulposus, annulus fibrosus (Fig. 1), and endplates (0.5-mm thick). The nucleus pulposus and annulus fibrosus were meshed utilizing hexahedral elements, and they occupied approximately 40% and 60% of the intervertebral disc volume, respectively.[4]

Mooney-Rivlin constitutive model was used to model the nonlinear behavior of the ground substance of both the nucleus pulposus and the annulus fibrosus. The annulus fibers, consisting of 8 layers, were modeled as hypoelastic materials using truss elements and were embedded within the annulus ground substance with an inclination of approximately 30° to the transverse plane.[18] Moreover, the main ligaments were established using nonlinear tension-only spring elements placed in their anatomically accurate positions, encompassing the anterior longitudinal ligament, posterior longitudinal ligament, ligamentum flavum, interspinous ligament, and facet capsular ligament[19,20] (Table 1).

3. Validation of the Intact FE Model

In the validation process, moments were applied to the rigid reference point of C2 vertebra in all FE models. The inferior surface of the T1 vertebrae was fully fixed in all degrees of freedom. For the intact C2–T1 model, we applied a 73.6 N follower load to the spine, followed by a 1.0-Nm moment on C2 vertebra for validation. The 73.6 N follower load represents a physiological axial compressive load to simulate the effect of head weight and muscle force.[12] The segmental ROMs of flexion, extension, lateral bending, and axial rotation were compared with experimental data from published literature.[21-23]

4. Establishment of the Surgical FE Models

The details of the established C5–6 ACDF model and the three 2-level RS models are shown in Fig. 2, and the surgical process is illustrated as follows. In all surgical segments of the surgical models, the intervertebral disc, anterior longitudinal ligaments, and posterior longitudinal ligaments were completely resected. After decompression, a cage plus ATLANTIS VISION Elite plate-screw system (Medtronic Sofamor Danek, Memphis, TN, USA), ZERO-P VA ZOP device (DePuy Syn-

https://doi.org/10.14245/ns.2347330.665

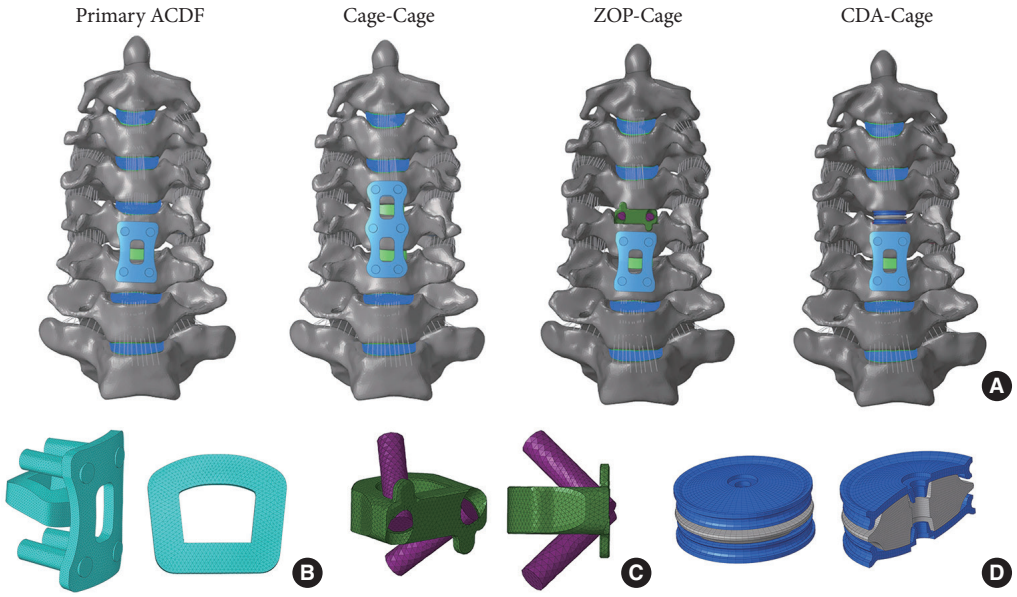

Fig. 2. Three-dimensional finite element (FE) models of C5–6 primary anterior cervical discectomy and fusion (ACDF) and revision surgery constructs were established. (A) Three-dimensional FE model of primary ACDF, Cage-Cage, ZOP-Cage, and CDA-Cage. Three-dimensional FE model of the cage plus plate (B), ZOP device (C), and Bryan artificial disc (D). ZOP, zero-profile; CDA, cervical disc arthroplasty.

thes, Raynham, MA, USA), or Bryan cervical disc (Medtronic Sofamor Danek) was implanted at the C4–5 segment, respectively. Both contact surfaces of the intervertebral devices were ensured to be in complete contact with the corresponding endplates, and the screw and plate were used to stabilize the surgical segments further.[15] In the C5–6 primary ACDF segment, polyetheretherketone cages filled with center bone graft (cancellous bone properties)[7,24] were inserted, followed by the placement of anterior titanium alloy plates (length 21 mm) and screws (insertion angle approximately 0°) to achieve solid fusion. The nodes within the interface region of the devices and bone were shared to connect them to the models. The material properties of different implant devices, including cage, screw plus plate, ZOP devices, and Bryan disc, are also listed in Table 1.

5. Loading Conditions of the Surgical Models

A follower load of 73.6 N and a pure moment of 1.0 Nm was imposed on the primary ACDF model to produce ROMs in 3 planes. All RS models, including Cage-Cage, ZOP-Cage, and CDA-Cage, were subjected to displacement loads; the displacement load applied to all RS models matched the total C2–T1 ROMs of the primary ACDF model. Soft and frictionless contact properties were used to replicate the sliding contact between the cartilage endplates of the facet joints.[25] Finally, the segmental ROM, IDP, and FJF in different surgical models during 3 motion planes were calculated. During extension, the mean FJFs for both left and right facet joints at the same level were recorded and calculated. The FJF during flexion was not calculated because the C2–T1 facet joints had no contact forces. The FJFs on the loaded side were recorded and then averaged for the left and right loading conditions.

RESULTS

1. Model Validation

In the present study, the segmental ROMs for C2–T1 in the intact model were compared with those from both *in vitro* studies and FE studies. During flexion-extension, the ROMs observed in the present study are close to the data from the *in vitro* study conducted by Wheeldon et al.[22] In the present study, segmental ROM is slightly higher at C4–5 and C6–7, exceeding 3° compared to the study of Erbulut et al.,[26] but similar in other segments (Fig. 3A).

During lateral bending, the ROMs of C2–3 and C7–T1 are close to the *in vitro* study by Yogananda et al.[23] and the FE studies by Wu et al.[27] and Wang et al.[28] In the C3–4, C4–5, and C5–6 segments, our study's ROM values are notably lower than those reported by Yogananda et al.[23] and Wang et al.[28] However, the difference is relatively smaller, approximately 1° or less, when compared to the data presented by Wu et al.[27] (Fig. 3B).

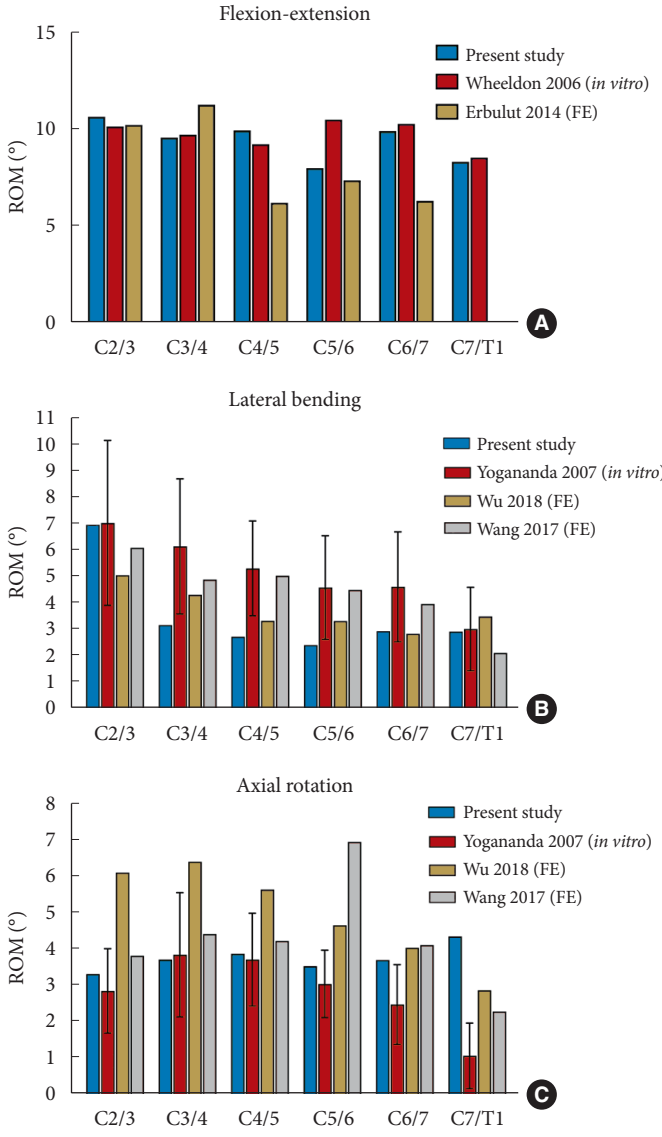

Fig. 3. Model validation of C2–T1 intact finite element (FE) model of the present study under a 1.0-Nm moment, compared with the published studies. (A–C) Comparison of segmental range of motions (ROMs) of C2–T1 during flexion-extension, lateral bending, and axial rotation.

Finally, the segmental ROM for axial rotation in this study was also compared with the data of the study conducted by Yogananda et al.,[23] Wu et al.,[27] and Wang et al.[28] Except for the C7–T1 segment, the segmental ROMs of the other segments exhibit close to at least 2 of the 3 studies referenced. Moreover, the ROM for the C7–T1 segment in the present study is higher than the 1.48° reported by Wu et al.[27] (Fig. 3C).

2. ROMs at the Adjacent Segments

Under a follower load of 73.6 N, the total C2–T1 ROMs in

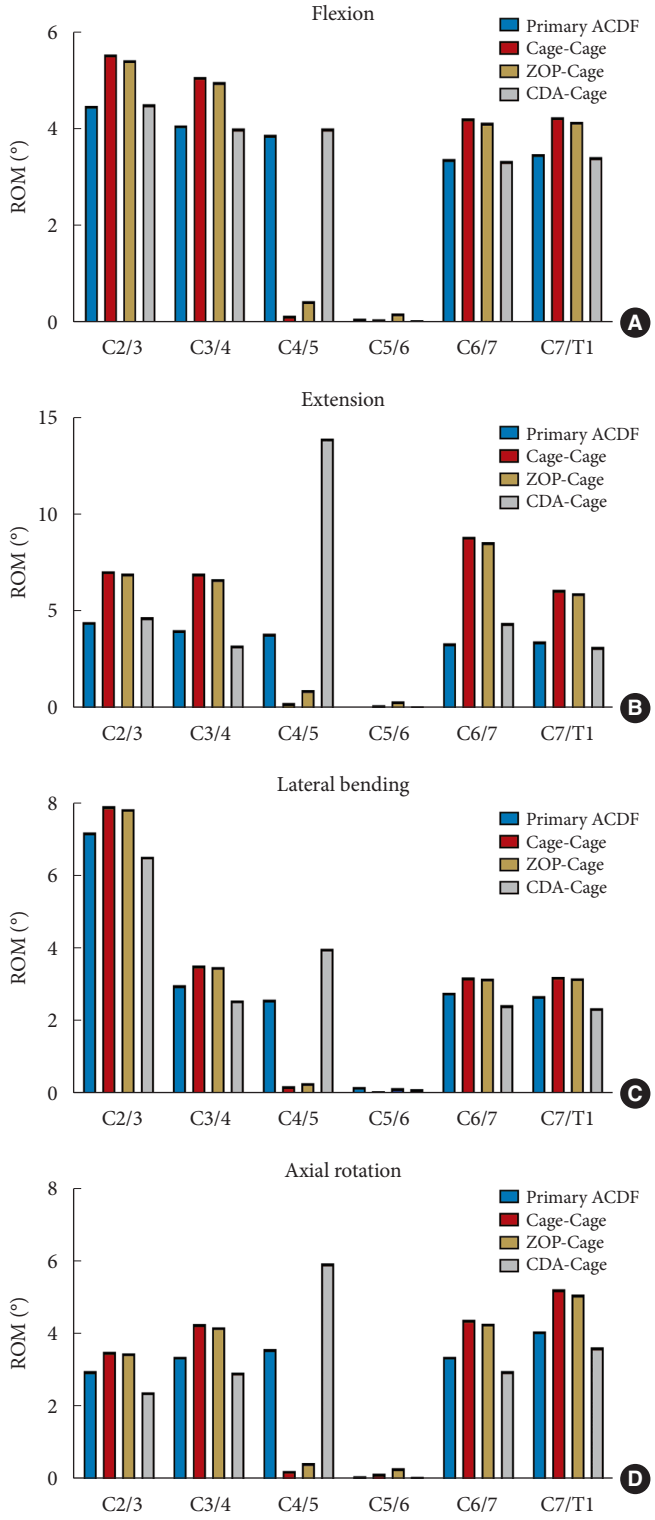

Fig. 4. Comparison of range of motions (ROMs) in different finite element models during flexion (A), extension (B), lateral bending (C), and axial rotation (D). ACDF, anterior cervical discectomy and fusion; ZOP, zero-profile; CDA, cervical disc arthroplasty.

https://doi.org/10.14245/ns.2347330.665

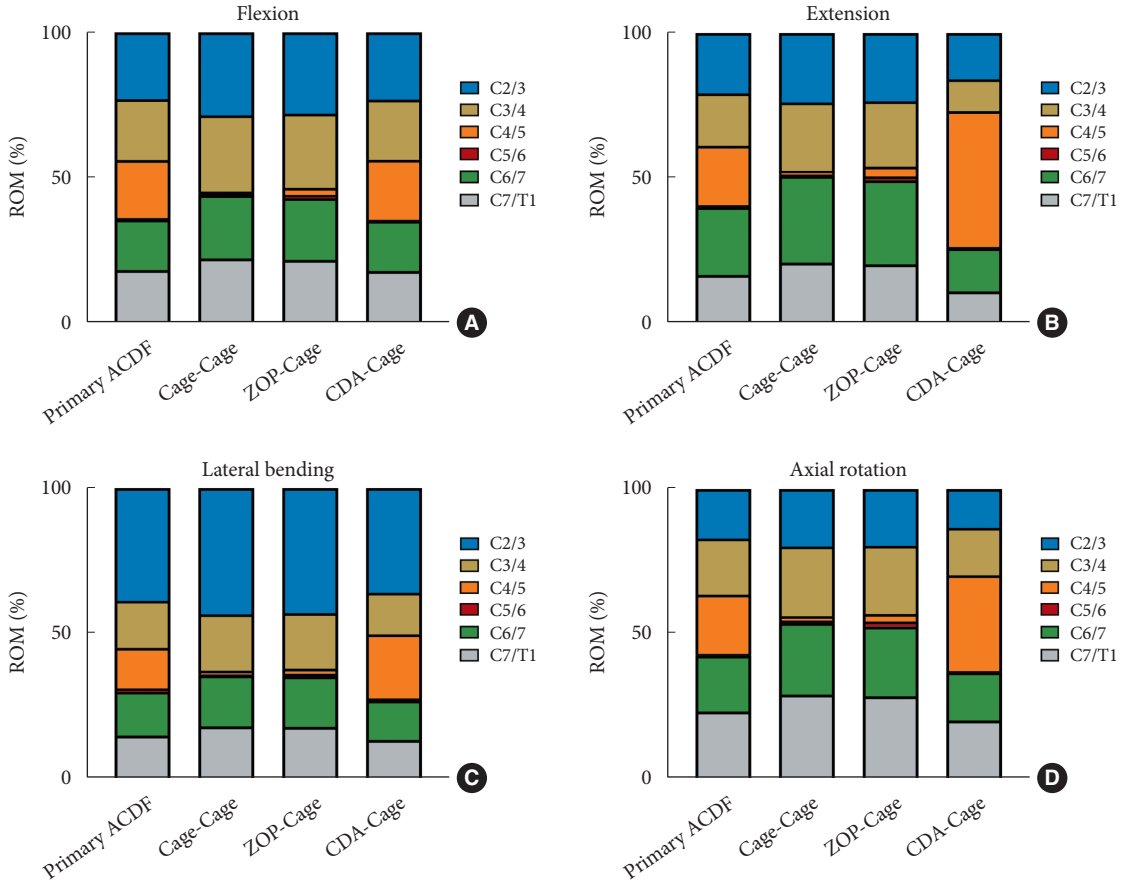

Fig. 5. Comparison of distribution percentage of the ROM in different finite element models during flexion (A), extension (B), lateral bending (C), and axial rotation (D). ACDF, anterior cervical discectomy and fusion; ZOP, zero-profile; CDA, cervical disc arthroplasty.

the primary ACDF model following a 1-Nm moment during flexion, extension, lateral bending, and axial rotation were 19.5°, 29.8°, 18.5°, and 17.6°, respectively. The total C2–T1 ROMs of all 3 RS models matched those of the primary ACDF model. Fig. 4 illustrates the segmental ROMs for the primary ACDF and 3 RS models in different motion directions. In comparison to the primary ACDF model, the ROMs of C3–4 and C6–7 adjacent segments of the Cage-Cage model and ZOP-Cage model were increased in all motion directions; and the ROMs of the ZOP-Cage model were lower than those of the Cage-Cage model in all motion directions. The CDA-Cage model has the lowest adjacent segment ROM among all RS models in all motion directions. Furthermore, the ROMs of the upper and lower adjacent segments in the CDA-Cage model were lower than those in the primary ACDF model during extension, lateral bending, and axial rotation, except for C6/7, while during flexion was close to those in the primary ACDF model.

3. Distribution Percentage of Segmental ROMs

The ROM percentages for each C2–T1 segment are shown in Fig. 5. In comparison to the primary ACDF model, both the Cage-Cage and ZOP-Cage models exhibited an increase in the ROM ratio of the C3–4 and C6–7 segments in all motion directions. The CDA-Cage model demonstrated the lowest ROM ratio of C3–4 and C6–7 segments among all RS constructs, which is close to or lower than those of the primary ACDF model in all motion directions. Additionally, the intervertebral ROM at the C4–5 segment in the CDA-Cage model was preserved and exhibited overactivity compared to the primary ACDF model during extension, lateral bending and axial rotation.

4. Segmental IDP Analysis at Adjacent Segments

The IDP of the adjacent segments in the different FE models are shown in Fig. 6. Among the RS models, the Cage-Cage model had the highest IDP in the C3–4 and C6–7 segments, followed by the ZOP-Cage model, both surpassing the primary ACDF

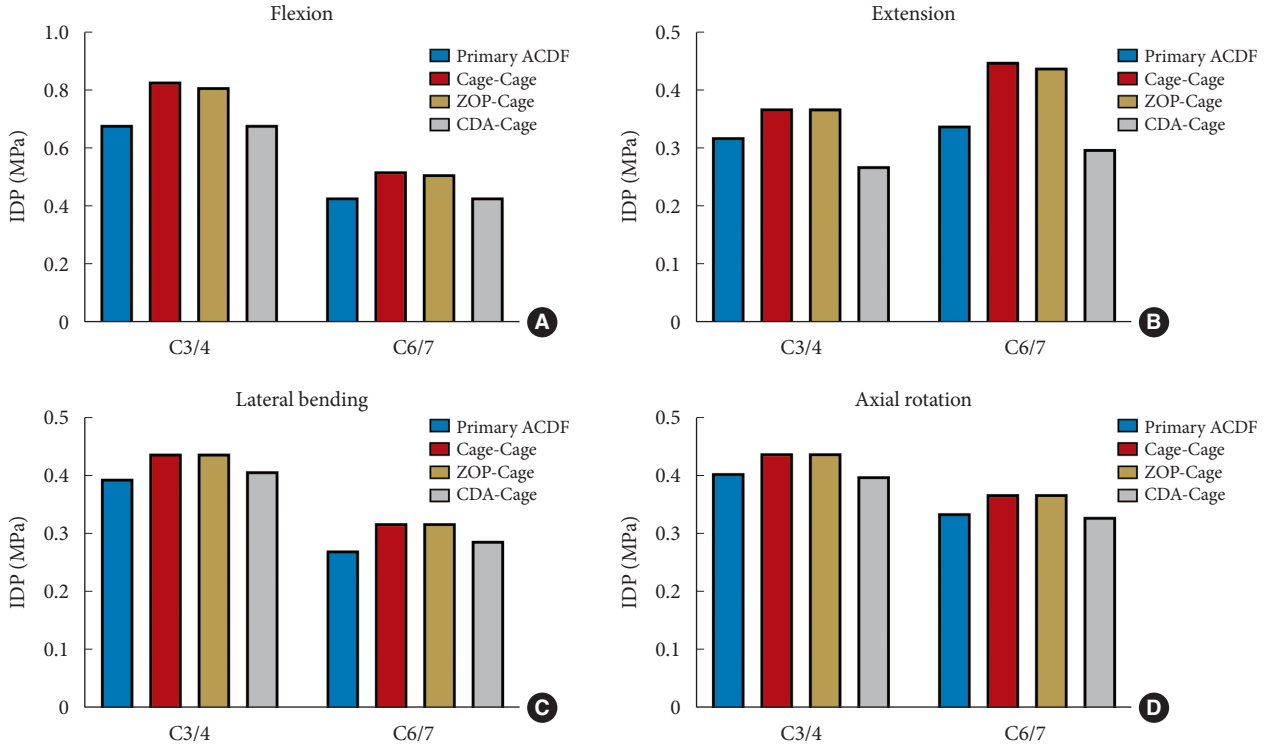

Fig. 6. Comparison of intradiscal pressure (IDP) at the upper and lower adjacent segments in different operation finite element models during flexion (A), extension (B), lateral bending (C), and axial rotation (D). ACDF, anterior cervical discectomy and fusion; ZOP, zero-profile; CDA, cervical disc arthroplasty.

model in all motion directions. The CDA-Cage model exhibited IDP values similar to the primary ACDF model. Specifically, during extension, the IDP in the C3–4 and C6–7 segments of the CDA-Cage model was lower than that of the primary ACDF model.

5. Stress Analysis of the Discs at Adjacent Segments

The disc stress distribution features of the C3–4 and C6–7 discs in each model are shown in Figs. 7 and 8, respectively. The maximum von Mises stresses of annulus fibrosus at the C3–4 and C6–7 discs were higher than those of the nucleus pulposus in all directions. In different motion directions, the maximum von Mises stress was concentrated at the loading side's corresponding edge. Comparing RS models to the primary ACDF model, the Cage-Cage and ZOP-Cage models exhibited increased maximum von Mises stress in C3–4 and C6–7 intervertebral discs. Conversely, the CDA-Cage model showed reduced maximum von Mises stress levels, except for the C6–7 segment during flexion.

6. FJF Analysis at Adjacent Segments

The FJF values of the different FE models in the upper and lower adjacent segments are presented in Fig. 9. In comparison to the primary ACDF model, the FJF values at the C3–4 and C6–7 levels in the Cage-Cage and ZOP-Cage models were increased, with the Cage-Cage model demonstrating the highest values, except at C3–4 during lateral bending. Moreover, the CDA-Cage model exhibited a reduced FJF values at the C3–4 and C6–7 segments in comparison to the primary ACDF model during extension, lateral bending and axial rotation.

DISCUSSION

1. Main Findings May Benefit the Decision-Making of ACDF RS

Cervical hybrid surgery is an effective method to preserve the ROM in cases of CDD, and it can effectively delay the process of cervical degeneration.[12] In the selection of internal fixators for ACDF surgery, ZOP devices exhibit clear advantages over traditional cage plus plate structures in terms of both clinical efficacy and biomechanical response reduction. This study innovatively compared the RS methods focusing on the hybrid CDA-Cage construct, as well as ACDF involving ZOP devices and traditional cage plus plate structures following primary

https://doi.org/10.14245/ns.2347330.665

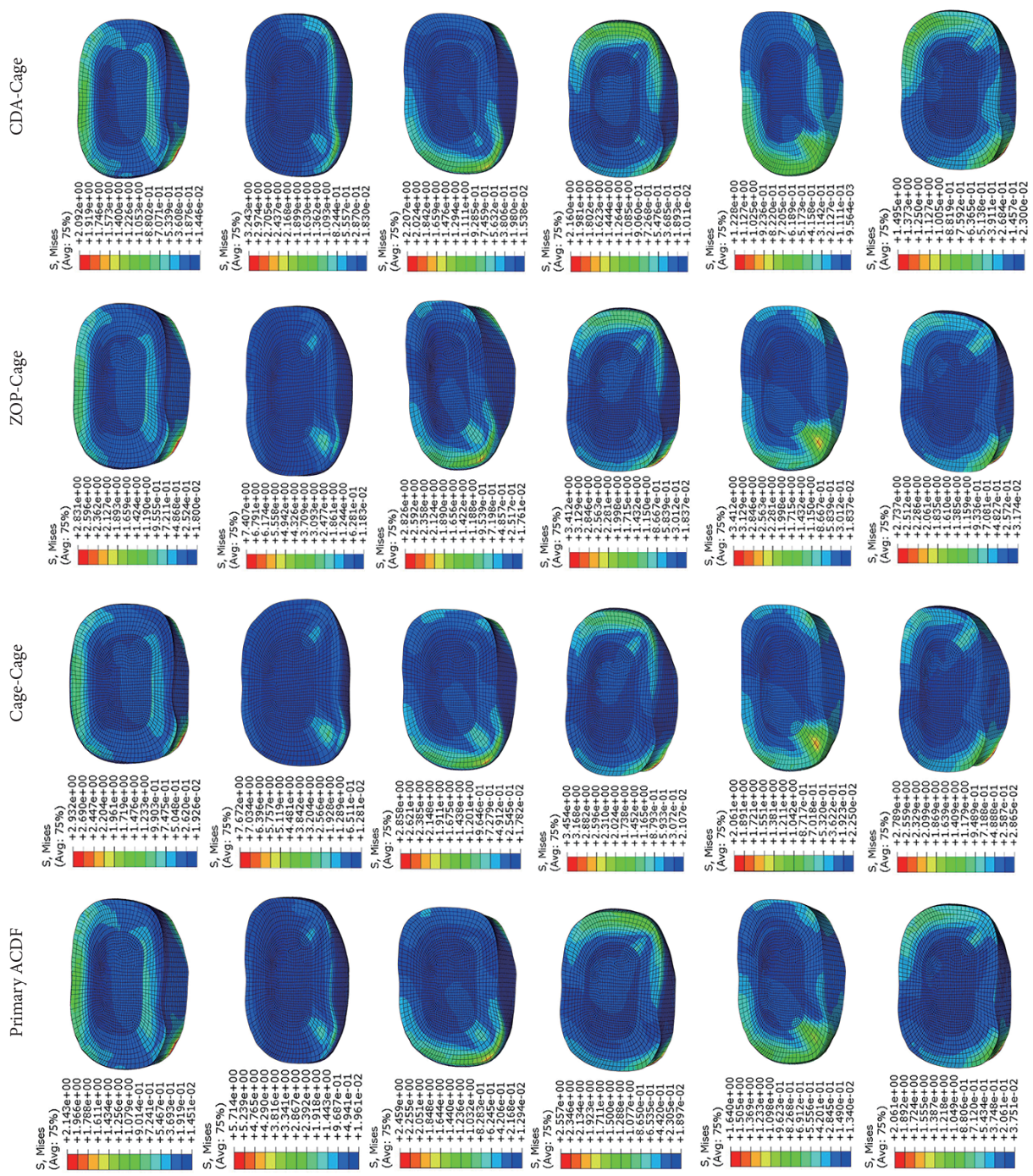

Fig. 7. The von Mises stress cloud map of C3–4 intervertebral disc in operation finite element (FE) models. Stress distribution characteristics of C3–4 intervertebral discs in different FE models during flexion, extension, left bending, right bending, left rotation, and right rotation were shown. ACDF, anterior cervical discectomy and fusion; ZOP, zero-profile; CDA, cervical disc arthroplasty.

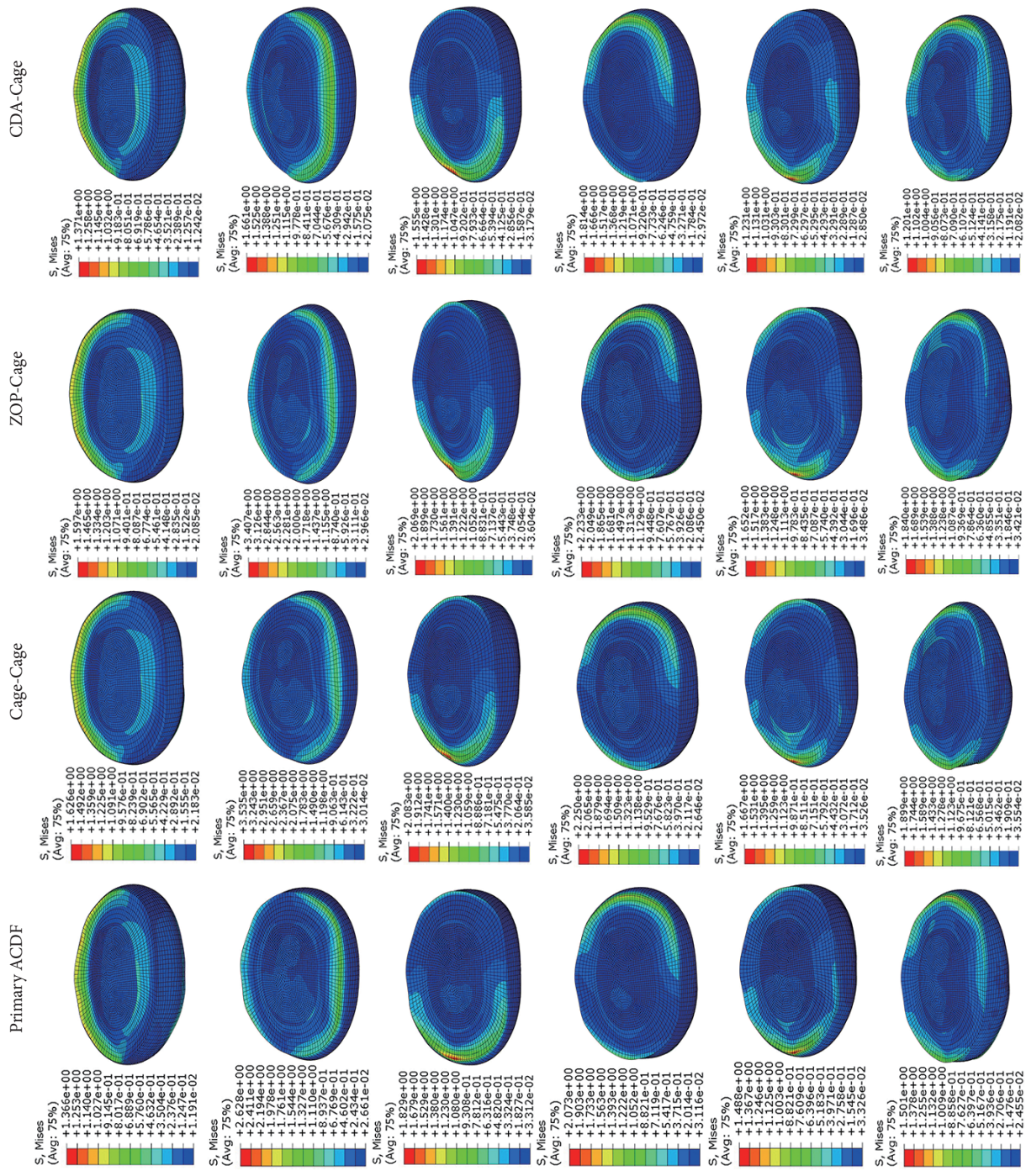

Fig. 8. The von Mises stress cloud map of C6–7 intervertebral disc in operation finite element (FE) models. Stress distribution characteristics of C6–7 intervertebral discs in different FE models during flexion, extension, left bending, right bending, left rotation, and right rotation were shown. ACDF, anterior cervical discectomy and fusion; ZOP, zero-profile; CDA, cervical disc arthroplasty.

https://doi.org/10.14245/ns.2347330.665

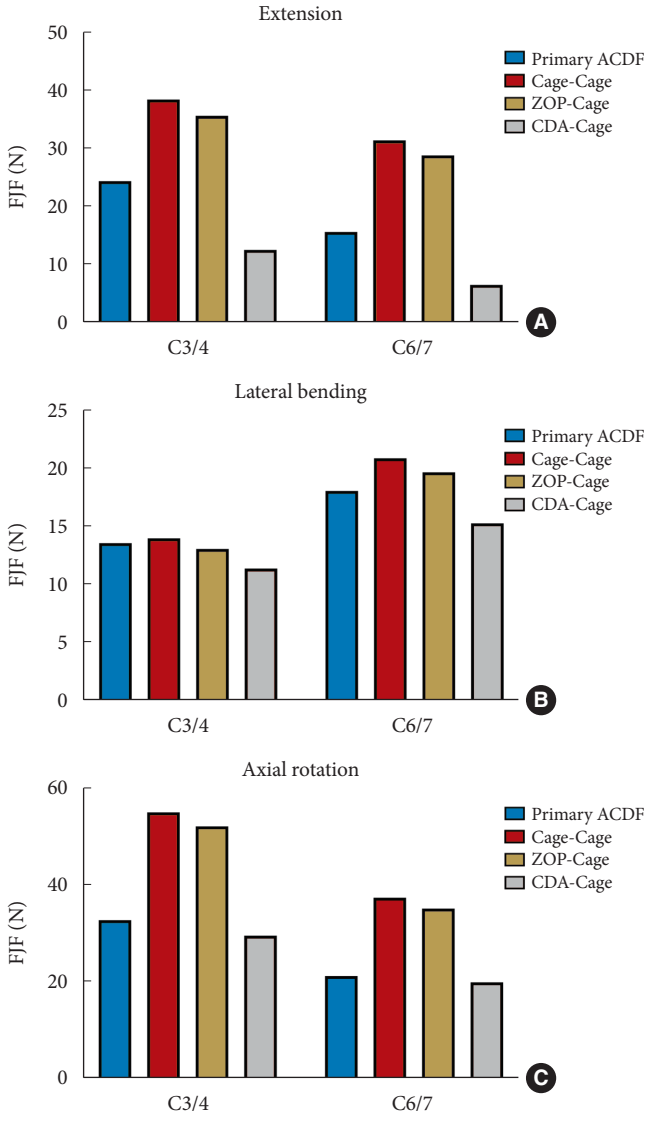

Fig. 9. Comparison of facet joint force (FJF) at the upper and lower adjacent segments in different operation finite element models during extension (A), lateral bending (B), and axial rotation (C). ACDF, anterior cervical discectomy and fusion; ZOP, zero-profile; CDA, cervical disc arthroplasty.

ACDF from the perspective of biomechanics. The authors established a C2–T1 intact model, in which the primary operation was conducted in the C5–6 segment that was most prone to degeneration in the clinic, while the RS addressed the C4–5 higher adjacent segment due to ASD. Using the 3 revision methods mentioned above, we systematically compared the changes in biomechanical responses of the upper and lower adjacent segments following different RS models. Our results indicated that both ZOP-Cage and CDA-Cage constructs reduced biomechanical responses, providing valuable data for guiding clinical decision-making when selecting surgical methods to minimize the risk of re-ASD after RS.

2. ROMs at Adjacent Segments and Distribution of Segmental ROMs

After ACDF, the loss of ROM in the fusion segment was compensated by other nonfusion segments.[15,29] These adjacent segments are most susceptible to biomechanical changes, exhibiting a significant increase in ROM and a higher risk of ASD. When different types of internal fixators were implanted in the surgical segment, the ROM compensation of the adjacent segments was different. In this study, compared to the Cage-Cage model, the ZOP-Cage model has a larger ROM, which results in a slightly smaller adjacent segmental ROM than the Cage-Cage model. When the ROMs of the surgical segments with CDA were all retained or even overactive, making CDA-Cage model has the lowest adjacent segment ROM among all RS models. These findings are in line with those of Faizan et al.,[30] which suggest that the adjacent segmental ROM, facet joint loads, and endplate stresses of CDA combined with ACDF were closer to the normal model than the 2-level ACDF model, and had less effect on the biomechanical responses of adjacent segments. Wong et al.[12] demonstrated that in the FE models of the three-level continuous hybrid surgery model, the reduction in ROM in the lower adjacent segment was at the cost of increased ROM in the upper adjacent segments. Additionally, Wu et al.[14] found that the location of ACDF and CDA is an important factor in the kinematics of adjacent segments, and the ROM of adjacent ACDF segments increases much more than that of adjacent CDA segments. However, our study is inconsistent with the findings of the 2 studies of Wong et al.[12] and Wu et al.,[14] and as we did not observe significantly higher or lower ROM in the C3–4 segment compared to the C6–7 segment in the CDA model. This discrepancy may be attributed to the number of total segments or surgical segments used in the study, as well as the location limitations of the surgical segment of the CDA imposed by revision. In this study, when compared to the other 2 RS models, the CDA-Cage model demonstrates the most significant reduction in ROM in the 2 adjacent segments. However, there were no significant differences observed in the reduction of ROM between the upper and lower adjacent segments in the CDA-Cage model. The effects of the number of total segment and hybrid segments in different models and the location of CDA and ACDF on adjacent ROMs still need to be further clarified.

3. IDP and Disc Stress Analysis at Adjacent Segments

The changes in IDP after ACDF may be attributed to many

factors, including patient-specific factors (such as head and neck gravity, neck muscle condition, and natural degenerative state of discs), the length of fused segments, and the type of internal fixation.[31] The rise in IDP obstructs the diffusion of nutrient substances from the endplate to the intervertebral disc, leading to a deterioration in the nutritional status of the disc. This is also considered a crucial factor contributing to disc degeneration in patients following fusion surgery for ASD.[32] An increased number of fusion segments is a high-risk factor for ASD after multilevel cervical fusion.[6] Patients who underwent multilevel fusion experienced a more substantial decrease in overall ROM and exhibited increased compensatory ROM in the upper adjacent segments. This increased ROM was associated with a higher IDP, which in turn elevated their risk of developing degeneration.[3]

Previous study has demonstrated that IDP in adjacent segments following 2-level continuous hybrid surgery is significantly lower than that following 2-level continuous ACDF surgery.[10] Our study found a consistent phenomenon in the hybrid CDA-Cage model exhibiting the lowest adjacent segmental IDP among the 3 RS models. Additionally, the present study also used a stress cloud map to display the distribution of von Mises stress on the disc. The stress cloud maps showed that the maximum stress on the disc concentrated at the corresponding edge of the loading side. Among all RS models, both Cage-Cage and ZOP-Cage models showed an increased maximum stress at the C3–4 and C6–7 intervertebral discs when compared to the primary ACDF model, whereas the CDA-Cage model consistently exhibited the lowest maximum stress. In the hybrid CDA-Cage model, the changes of IDP and maximum disc stress in adjacent segments are close to the trends observed in ROM and FJF during different postures, suggesting that CDA has a significant protective effect on the disc of both adjacent segments.

4. FJF Analysis at Adjacent Segments

Hypermobile facet joints in adjacent segments following cervical fusion can lead to increased stress load, potentially resulting in cervicogenic neck pain and even headaches.[33] ACDF induces a decrease in FJF within the fusion segment due to rigid fixation. Studies have demonstrated that the implantation of an artificial intervertebral disc keeps the operative segment from overloading the facet joints and keeps them in a relatively healthy state.[34] The Bryan disc used in this study has been found to reduce FJFs at the surgical segments, potentially delaying facet joint degeneration and lowering the associated degenerative risk. Conversely, other clinically used discs such as Mobi-C and Prestige-LP discs have shown an increased FJF.[35] In addition to the FJF of the operative segment, the bearing load by facet joints of adjacent segments plays a pivotal role in predicting degeneration. Our study showed that the FJF at adjacent segments of both Cage-Cage and ZOP-Cage constructs increased compared with the primary ACDF model. In contrast, FJF in adjacent segments of CDA-Cage hybrid constructs exhibited a significant decrease compared to the primary ACDF model. The changes in FJF in adjacent segments were consistent with the changes in ROM, with CDA-Cage constructs demonstrating a positive biomechanical effect in preventing facet joint degeneration. Faizan et al.[30] found that CDA can protect adjacent facet joints by compensating for ROM, resulting in a tendency for increased facet joint load at the CDA level while not significantly increasing FJF at adjacent segments. This phenomenon was also corroborated in our model, as FJF in the adjacent segments above the CDA level was lower than that in the CDA-operated segment. Previous studies have shown that the increase in contact force and load of adjacent facet joints after fusion surgery may lead to pathological injuries of the articular surface and ultimately accelerate joint surface degeneration.[36,37] In this study, CDA effectively alleviates adjacent segment FJF, thereby mitigating ASD and providing an effective means to alleviate neck pain resulting from facet joint hypermobility.

5. Summary Analysis of Biomechanical Parameters Combined With Clinical Application

From a biomechanical perspective, our study reveals that in the RS methods, the hybrid CDA-Cage construct provides superior protection for adjacent segments compared to both ZOP-Cage and Cage-Cage constructs. Among the 3 RS constructs, CDA-Cage performed the most significant reduction in ROM, IDP, maximum disc stress, and FJF at the adjacent segments. Because of the large number of patients undergoing revision due to ASD after 1-level ACDF, the results of this study can be used as a reference for surgeons when determining the optimal approach (CDA-Cage or ZOP-Cage) for single-stage ACDF revision. Due to the relatively strict surgical indications of CDA, the hybrid CDA-Cage construct is recommended as the preferred surgical approach in patients not involving severe osteoporosis, severe cervical instability, trauma, or pathological bone injury.[38,39] For the clinical effect, hybrid surgery exhibited the advantages of less intraoperative blood loss, shorter return duration to work, and a lower incidence of nerve injury.[17] For patients who do not meet CDA criteria, ZOP-Cage emerges as a superior surgical choice over Cage-Cage, and both of these op-

 https://doi.org/10.14245/ns.2347330.665

erations can meet the need for strong fixation of the cervical spine.[4]

6. Limitations

The present study has several limitations. Firstly, the cervical spine FE model was generated based on the cervical spine of a single healthy individual, and related data could not be analyzed statistically between groups. Simple biases that occur during model construction may have a small impact on biomechanical response parameter trends. Secondly, while the plate-screw system, ZOP device and artificial disc used in this study have been proven to have good representativeness and clinical effects, they may still differ from other products of the same category. For example, the biomechanically distinctive ZEVO plate-screw system (Medtronic Sofamor Danek) with short plates and high-angled screws has demonstrated superior mechanical stability and load-sharing capabilities.8 Furthermore, it has shown efficacy in effectively preventing cage subsidence and reducing adjacent-level ossification development.[5] Given its proven advantages, future comparative research should incorporate this short plate-high-angled screw system, along with the different cortico-cancellous composition of allograft spacers. The generalizability of the study's conclusions to other similar products requires further validation. Thirdly, some common cervical degenerative manifestations (osteophytic hyperplasia, disc, facet joints, endplate degenerative injuries) were not simulated in this study because this study focuses more on the comparison of different revision procedures. Future studies are needed to investigate the different material properties of degeneration and plate fixation as RS for biomechanically assuming the risk of ASD.

CONCLUSION

In this FE study, the biomechanical responses on the adjacent segments of the CDA-Cage constructs were significantly lower than those of Cage-Cage and ZOP-Cage constructs with decreased ROM, IDP, maximum disc stress, and FJF. Moreover, CDA-Cage exhibited the best performance in reducing IDP and FJF at segments C3–4 and C7–T1. The CDA in hybrid CDA-Cage constructs reduces the biomechanical responses of the adjacent segments, making it the preferred revision procedure for preventing ASD. When patients do not meet the indications for CDA, the ZOP-Cage construct, with its superior biomechanical performance, can provide a more favorable alternative to traditional Cage-Cage constructs for preventing ASD. Further biomechanical and clinical studies are anticipated to investigate the effects of multilevel hybrid revision after ACDF surgery and to assess the impact of the relative positioning of CDA and ACDF on the biomechanics of adjacent segments. This study offers a reference for surgical decision-making based on biomechanical evidence regarding the use of hybrid surgery for the treatment of ASD following primary ACDF. It is necessary for future research to validate these conclusions.

NOTES

Conflict of Interest: The authors have nothing to disclose.

Funding/Support: This study is supported by the Beijing Hospitals Authority Youth Programme (No. QML20230315), Beijing Natural Science Foundation (No. 7242061), and Clinical Research Incubation Project, Beijing Chaoyang Hospital, Capital Medical University (No. CYFH202322).

Author Contribution: Conceptualization: WL, BH, YY, DS, PY, YH; Data curation: WL, BH, YY, DS, PY, YH; Formal analysis: WL, BH, YY, DS, PY, YH; Funding acquisition: PY, YH; Methodology: WL, YY, DS, PY, YH; Project administration: PY, YH; Visualization: WL, BH, PY, YH; Writing – original draft: WL, BH, YY; Writing – review & editing: WL, YY, PY, YH.

ORCID

Weishi Liang: 0000-0003-3565-6504
Bo Han: 0000-0002-3618-5700
Yihan Yang: 0009-0005-8254-8567
Duan Sun: 0009-0009-2374-2756
Peng Yin: 0000-0001-9984-7663
Yong Hai: 0000-0002-7206-325X

REFERENCES

1. Wu JC, Chang HK, Huang WC, et al. Risk factors of second surgery for adjacent segment disease following anterior cervical discectomy and fusion: a 16-year cohort study. Int J Surg 2019;68:48-55.
2. Carrier CS, Bono CM, Lebl DR. Evidence-based analysis of adjacent segment degeneration and disease after ACDF: a systematic review. Spine J 2013;13:1370-8.
3. Shin JJ. Comparison of adjacent segment degeneration, cervical alignment, and clinical outcomes after one- and multilevel anterior cervical discectomy and fusion. Neurospine 2019;16:589-600.
4. Hua W, Zhi J, Ke W, et al. Adjacent segment biomechanical

changes after one- or two-level anterior cervical discectomy and fusion using either a zero-profile device or cage plus plate: a finite element analysis. Comput Biol Med 2020;120:103760.
5. Jimenez KA, Kim J, Lee J, et al. Short plate with screw angle over 20 degrees improves the radiologic outcome in ACDF: clinical study. J Clin Med 2021;10:2034.
6. Broida SE, Murakami K, Abedi A, et al. Clinical risk factors associated with the development of adjacent segment disease in patients undergoing ACDF: a systematic review. Spine J 2023;23:146-56.
7. Ke W, Chen C, Wang B, et al. Biomechanical evaluation of different surgical approaches for the treatment of adjacent segment diseases after primary anterior cervical discectomy and fusion: a finite element analysis. Front Bioeng Biotechnol 2021;9:718996.
8. Kwon JW, Bang SH, Kwon YW, et al. Biomechanical comparison of the angle of inserted screws and the length of anterior cervical plate systems with allograft spacers. Clin Biomech (Bristol, Avon) 2020;76:105021.
9. Wang Z, Zhu X, Wang Z, et al. Zero-P and ROI-C implants versus traditional titanium plate with cage to treat cervical spondylotic myelopathy: clinical and radiological results with 5 years of follow-up. BMC Musculoskelet Disord 2023;24:539.
10. Hua W, Zhi J, Wang B, et al. Biomechanical evaluation of adjacent segment degeneration after one- or two-level anterior cervical discectomy and fusion versus cervical disc arthroplasty: a finite element analysis. Comput Methods Programs Biomed 2020;189:105352.
11. Lu VM, Zhang L, Scherman DB, et al. Treating multi-level cervical disc disease with hybrid surgery compared to anterior cervical discectomy and fusion: a systematic review and meta-analysis. Eur Spine J 2017;26:546-57.
12. Wong CE, Hu HT, Hsieh MP, et al. Optimization of three-level cervical hybrid surgery to prevent adjacent segment disease: a finite element study. Front Bioeng Biotechnol 2020;8:154.
13. Khalaf K, Nikkhoo M. Comparative biomechanical analyses of lower cervical spine post anterior fusion versus intervertebral disc arthroplasty: a geometrically patient-specific poroelastic finite element investigation. J Orthop Translat 2022;36:33-43.
14. Wu TK, Meng Y, Liu H, et al. Biomechanical effects on the intermediate segment of noncontiguous hybrid surgery with cervical disc arthroplasty and anterior cervical discectomy and fusion: a finite element analysis. Spine J 2019;19:1254-63.
15. Liang W, Han B, Hai Y, et al. Biomechanical analysis of the reasonable cervical range of motion to prevent non-fusion segmental degeneration after single-level ACDF. Front Bioeng Biotechnol 2022;10:918032.
16. Mumtaz M, Mendoza J, Vosoughi AS, et al. A comparative biomechanical analysis of various rod configurations following anterior column realignment and pedicle subtraction osteotomy. Neurospine 2021;18:587-96.
17. Lu T, Ren J, Sun Z, et al. Relationship between the elastic modulus of the cage material and the biomechanical properties of transforaminal lumbar interbody fusion: a logarithmic regression analysis based on parametric finite element simulations. Comput Methods Programs Biomed 2022;214:106570.
18. Kallemeyn N, Gandhi A, Kode S, et al. Validation of a C2-C7 cervical spine finite element model using specimen-specific flexibility data. Med Eng Phys 2010;32:482-9.
19. Mattucci SF, Moulton JA, Chandrashekar N, et al. Strain rate dependent properties of younger human cervical spine ligaments. J Mech Behav Biomed Mater 2012;10:216-26.
20. Sun Z, Lu T, Li J, et al. A finite element study on the effects of follower load on the continuous biomechanical responses of subaxial cervical spine. Comput Biol Med 2022;145:105475.
21. Panjabi MM, Crisco JJ, Vasavada A, et al. Mechanical properties of the human cervical spine as shown by three-dimensional load-displacement curves. Spine (Phila Pa 1976) 2001;26:2692-700.
22. Wheeldon JA, Pintar FA, Knowles S, et al. Experimental flexion/extension data corridors for validation of finite element models of the young, normal cervical spine. J Biomech 2006;39:375-80.
23. Yoganandan N, Pintar FA, Stemper BD, et al. Level-dependent coronal and axial moment-rotation corridors of degeneration-free cervical spines in lateral flexion. J Bone Joint Surg Am 2007;89:1066-74.
24. Kwon JW, Lee HM, Park TH, et al. Biomechanical analysis of allograft spacer failure as a function of cortical-cancellous ratio in anterior cervical discectomy/fusion: allograft spacer alone model. App Sci 2020;10:6413.
25. Mo Z, Zhao Y, Du C, et al. Does location of rotation center in artificial disc affect cervical biomechanics? Spine (Phila Pa 1976) 2015;40:E469-75.
26. Erbulut DU, Zafarparandeh I, Lazoglu I, et al. Application of an asymmetric finite element model of the C2-T1 cervical spine for evaluating the role of soft tissues in stability. Med

 https://doi.org/10.14245/ns.2347330.665

Eng Phys 2014;36:915-21.
27. Wu WK, Yan ZJ, Zhang TF, et al. Biomechanical influences of transcorporeal tunnels on C4 vertebra under physical compressive load under flexion movement: a finite element analysis. World Neurosurg 2018;114:e199-208.
28. Wang K, Wang H, Deng Z, et al. Cervical traction therapy with and without neck support: a finite element analysis. Musculoskelet Sci Pract 2017;28:1-9.
29. Tan LA, Yoganandan N, Choi H, et al. Biomechanical analysis of 3-level anterior cervical discectomy and fusion under physiologic loads using a finite element model. Neurospine 2022;19:385-92.
30. Faizan A, Goel VK, Biyani A, et al. Adjacent level effects of bi level disc replacement, bi level fusion and disc replacement plus fusion in cervical spine--a finite element based study. Clin Biomech (Bristol, Avon) 2012;27:226-33.
31. Weinhoffer SL, Guyer RD, Herbert M, et al. Intradiscal pressure measurements above an instrumented fusion. A cadaveric study. Spine (Phila Pa 1976) 1995;20:526-31.
32. Bowden JA, Bowden AE, Wang H, et al. In vivo correlates between daily physical activity and intervertebral disc health. J Orthop Res 2018;36:1313-23.
33. Malhotra A, Pace A, Ruiz Maya T, et al. Headaches in hypermobility syndromes: a pain in the neck? Am J Med Genet A 2020;182:2902-8.
34. Bauman JA, Jaumard NV, Guarino BB, et al. Facet joint contact pressure is not significantly affected by ProDisc cervical disc arthroplasty in sagittal bending: a single-level cadaveric study. Spine J 2012;12:949-59.
35. Yoganandan N, Purushothaman Y, Choi H, et al. Biomechanical effects of uncinate process excision in cervical disc arthroplasty. Clin Biomech (Bristol, Avon) 2021;89:105451.
36. Ke S, He X, Yang M, et al. The biomechanical influence of facet joint parameters on corresponding segment in the lumbar spine: a new visualization method. Spine J 2021;21:2112-21.
37. Li XF, Lv ZD, Yin HL, et al. Impact of adjacent pre-existing disc degeneration status on its biomechanics after single-level anterior cervical interbody fusion. Comput Methods Programs Biomed 2021;209:106355.
38. Patel N, Abdelmalek G, Coban D, et al. Should patient eligibility criteria for cervical disc arthroplasty (CDA) be expanded? A retrospective cohort analysis of relatively contraindicated patients undergoing CDA. Spine J 2024;24:210-8.
39. Berry KM, Govindarajan V, Berger C, et al. Effects of obesity on cervical disc arthroplasty complications. Neurospine 2023;20:1399-406.